Second Conference on Smart Monitoring,
Assessment and Rehabilitation of Civil Structures

SMAR 2013

Experimental characterization of fiber optic sensors embedded in CFRP materials

Antonio Brancaccio[1], Raffaella Di Sante[2], Lorenzo Donati[2] and Filippo Bastianini[3]

[1] SGM Experimental Engineering, Perugia, Italy
[2] Dpt. Of Engineering for Industry DIN, Forlì, Italy
[3] SestoSensor srl, Bologna, Italy

ABSTRACT: This paper describes the application of the optical low-coherence reflectometry technique (OLCR) to the estimation of optical losses in optical fibers and fiber Bragg grating sensors embedded into CFRP material specimens. Based on the use of an ASE tunable narrowband light source coupled to a Michelson interferometer, it was possible to evaluate both the concentrated and the distributed loss with high spatial resolution for different CFRP materials, fiber coatings and fiber type. In particular, prepreg unidirectional and twill 2x2 weave CFRP material were used for the manufacturing of the specimens, acrylate- and polyimide-coated standard fibers and bend-insensitive fibers were embedded and tested by using the OLCR technique. As a result, it was possible to locate and identify the sources of optical loss introduced by the CFRP manufacturing process and the technological solutions adopted to embed the fibers into the material.

1 INTRODUCTION

Optical fiber sensors[1-6] have gained great popularity for in-service static and dynamic strain monitoring of civil structures due to a series of advantages over more traditional gauges, e.g. immunity to electromagnetic interference, multiplexing and long-term installation, small dimensions, resistance to corrosion. In addition, optical fibers offer the possibility to embed the sensors in the material and therefore to realize a smart structure. Even if the integration of an optical fiber into the CFRP (Carbon Fiber Reinforced Polymers) material appears straightforward in principle due to the small dimensions of the fibers and their resistance, in practice the manufacturing process for industrial production of composite structures introduces a number of possible drawbacks due to mechanical and thermal stresses that may damage the fibers and the sensors or alter significantly their performance[6, 7]. This work has been carried out to investigate and estimate optical losses related to the CFRP manufacturing process by means of the optical low-coherence reflectometry technique (OLCR), which allows a much better spatial resolution with respect to the normally used optical time domain reflectometry (OTDR). This type of information plays an important role for accurate and reliable measurements with optical fiber sensors embedded into composite structures for in-service monitoring.

2 MATERIALS AND METHODS

2.1 Optical low-coherence reflectometer

Interferometric measurements of the fibers and sensors were performed using an ANDO AQ7410 with a Er3+ Amplified Spontaneous Emission (ASE) low-coherence laser source and a Michelson interferometer. As shown schematically in Figure 1, the wideband optical output from the light source is launched into a beam splitter and divided into two light beams. One beam is incident into the fiber under test, whereas the other beam is used as a local oscillator (LO) light through an optical delay line consisting of moving mirrors and reflectors. Light reflected back from the fiber under test is combined with light from the LO and the interferogram produced is detected by a square-law detector when these path lengths are equalized. The reflection location along the optical waveguide is varied by changing the moving mirror position and the reflectivity is obtained from the intensity of the interference signal. Based on the capability of filtering to limit the actual bandwidth of the low-coherence source, with this instrument it is possible to give an estimation of the optical losses exactly around the wavelength of interest for the embedded FBG sensors. This type of reflectometer allows fast measurements of the return loss with high spatial resolution (0.15 mm@1550 nm and 0.70@1550 nm in narrow band mode) and the measurement of the Rayleigh backscattered light, which in turn enables the identification of the optical loss distribution due to dispersion along the optical waveguide.

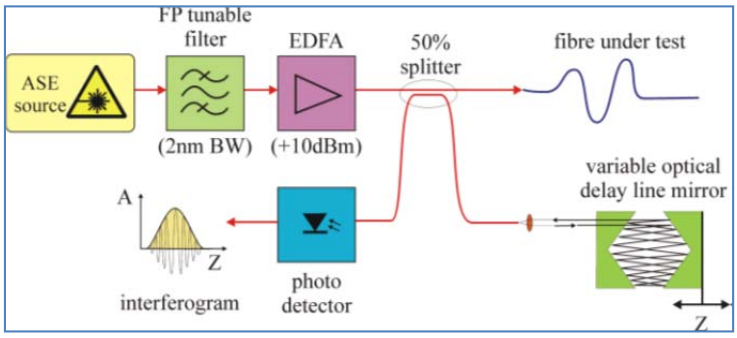

Figure 1. Basic detection scheme of the optical low-coherence reflectometer (OLCR) used in this work.

2.2 CFRP specimens

Small composite samples with embedded FBGs were produced by means of the vacuum bag technique at a temperature of 95°C or 120°C and a pressure of 3 bar in autoclave. The process had a duration of 8 hours at 95°C and of 1.5 hours at 120°C. The material used was a typical pre-preg material (MTM 57 T700S type, with thickness of 0.12 mm and specific weight of 150 g/mm^2), unidirectional. In the specimens, the plies were laid down at 0° and 90° according to the sequence [0°, 90°, 90°, 0°, 90°]2s. The resin used is a MTM 57 type. Figure 2 shows one of the specimens, which were shaped according to the ASTM 3039 standard for tensile tests. All specimens had a surface-mounted electrical strain gage and were subjected to tensile test in order to obtain useful information regarding their actual strain detection performance when embedded[8]. All the entry and egress points of the fibers in and out of the material were protected using small Sterling type sleeves or PTFE foils.

A second type of specimen was produced with embedded optical fibers without gratings, under the form of the composite boat mast section shown in Figure 3. The section has an elliptical shape of 140 mm and 60 mm maximum and minimum diameter respectively, is 1500 mm long

and 3,5 mm thick. In this case, six layers of Delta-Preg GG630-DT120-37 prepreg (twill 2x2, 12K Toray T700, toughened epoxy resin) were used, layered all along the 0° of the mast length. Two standard SMF-28e and two bend-insensitive fibers fully compliant with the ITU-T G.652.A1 standard specification were embedded along the specimen length between the outer layers, as visible in Figure 3. The manufacturing process was carried out in autoclave at a temperature of 90°C and a pressure of 3 bar, for 10 hours. Nylon "Sterling" sleeves and steel reinforced sheaths were used in order to protect the fibers at the ingress/egress points.

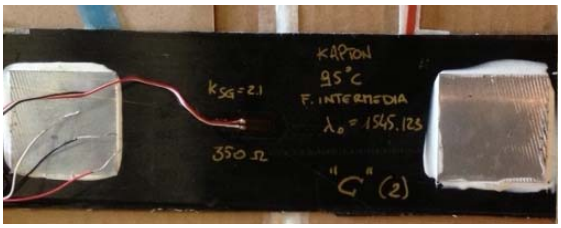

Figure 2. Composite sample produced at 95°C temperature and 3 bar pressure, with one embedded polyimide-coated FBG and a surface-mounted electrical strain gage.

Figure 3. Mast section with embedded fibers.

3 RESULTS AND DISCUSSION

All specimens were tested using the optical low-coherence reflectometer, both for the return loss at 1550 nm and for the loss distribution estimation. Figure 4 shows the results in terms of loss distribution obtained in the case of CFRP specimens with embedded acrylate and polyimide fiber Bragg gratings, whereas Figure 5 reports the distribution of the return loss for the same fibers and sensors. The results are plotted in the diagrams with reference to the distance from the optical connection port, reported on the horizontal axis. On the left side of the plots in Figure 4 and 6, higher peaks indicating concentrated losses are observed in the points where the fiber enters the material while shorter and generally wider peaks correspond to the locations where the protecting material ("Sterling" sleeve or PTFE foil) ends. The concentrated losses that are clearly detected are due to the high pressure (3 bar) employed during the manufacturing process in autoclave, which causes effects such as local bending of the fiber and changes in the refractive index, resulting in both the dispersion and the back-reflection of light into the waveguide. In the case of the polyimide fiber, these losses are reduced as a consequence of the improved high temperature resistance effect of this type of coating. Higher peaks on the right side of the plots correspond to the fiber termination, i.e. where the unprotected fiber actually ends due to breaking at the material-air interface. In neither case the Bragg peak of the embedded gratings appears wider as a possible result of the stress introduced by the curing cycle which may introduce non-uniform transverse and longitudinal strain and, as a consequence, distort the Bragg spectrum and causing the peak detection algorithm to fail in identifying the wavelength related to the pure longitudinal strain. In the case of the mast section, results are shown in Figure 6 for one of the two standard SMF28e fibers and in Figure 7, concerning one of the two G.652.A1 bend-insensitive fibers.

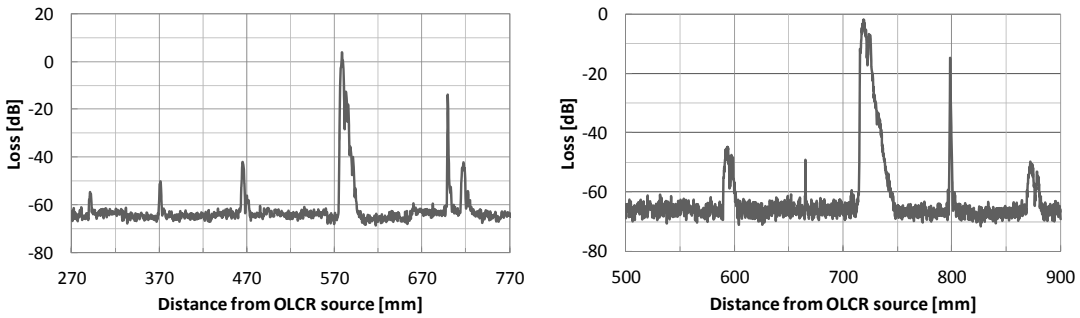

Figure 4. Dispersion in specimens with embedded polyimide-coated (left) and acrylate-coated (right) fibers and sensors.

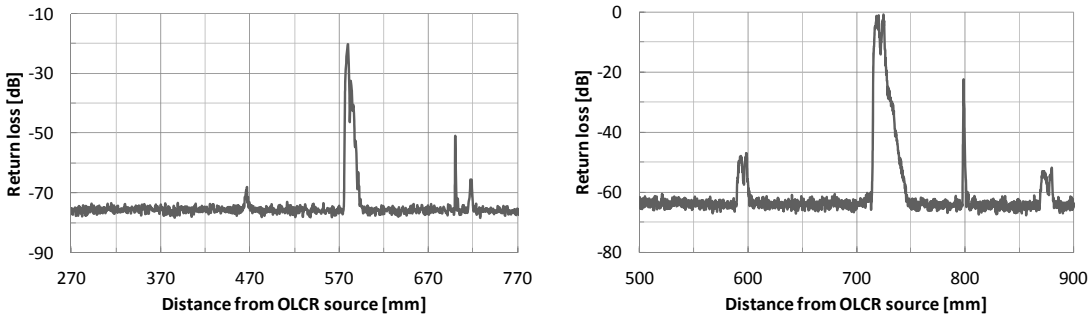

Figure 5. Reflectance in specimens with embedded polyimide-coated (left) and acrylate-coated (right) fibers and sensors.

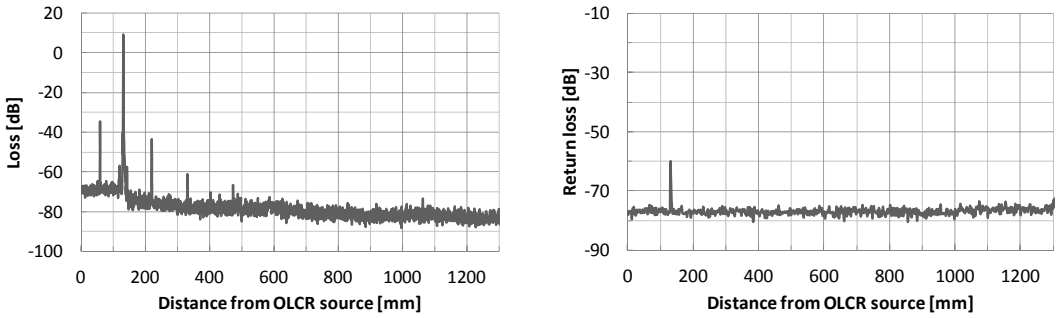

Figure 6. Dispersion (left) and reflectance (right) in SMF28 fiber embedded in the mast section.

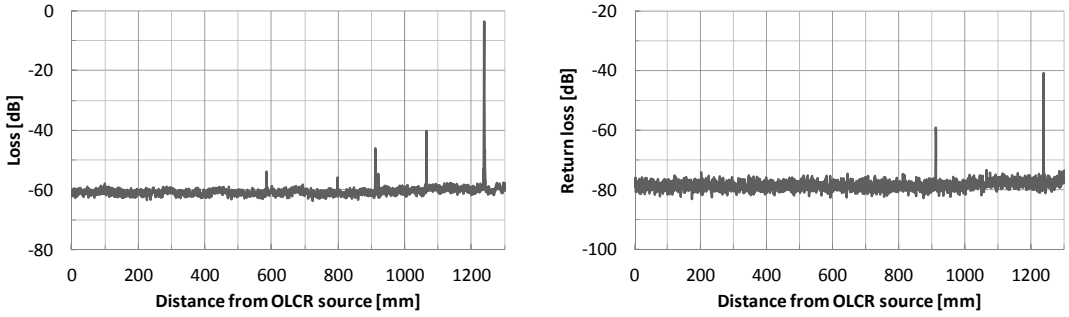

Figure 7. Dispersion (left) and reflectance (right) in bend-insensitive fiber embedded in the mast section.

It is clearly evident that while the SMF28e fiber suffers from heavy distributed loss and microbending damages at the fiber entry point in the material, the G.652.A1 bend-insensitive fiber does not. On longer samples than those investigated at first and described previously in this paper, the distributed loss is higher and is represented in Figure 6 by the decay of the baseline loss trace after the high peak on the left-hand plot. No sensible decreasing of the backscattering trace is instead visible in Figure 7, where the loss distribution in the bend-insensitive fiber is shown. Also, the peak related to the location where the SMF28e fiber enters the CFRP material, which is the highest peak at around 120 mm location in Figure 6, is no more evident when the bend insensitive fiber is used.

The transmission loss of the two fibers has also been approximately evaluated using the AQ7410 leveled ASE source and a Kingfisher H3 optical power meter. The transmission loss which however comprises the additional losses introduced by the optical connectors and the splices, was found to be 8.4 dB for the SMF28e fiber and only 0.25 dB for the G.652.A1 bend-insensitive fiber.

4 CONCLUSIONS

In this work, optical losses in fibers and gratings embedded in CFRP material specimens have been analyzed with high spatial resolution by using the optical low-coherence reflectometry technique (OLCR). The results obtained highlight how the points where the optical fiber enters and exit the FRP sample are the most critical locations for the arising of microbending losses due to the stresses of the curing process. Although it has been shown in this work that the protection of entry points with soft sleeves can mitigate the problem and achieve tolerable attenuation levels, the improvement of the fiber/CFRP transitions is believed to be a primary issue for allowing the application of fiber optic sensors on CFRP industrial products and for this reason it will be further investigated in future research work. A further result of this work suggests how bend-insensitive fibers can greatly reduce both the microbending losses at the FRP/bare fiber transition points and the distributed losses within the embedded length of the fiber. By combining the use of bend-insensitive fibers with the protection of the CFRP/bare fiber transition points the embedding of optical fiber sensors had been demonstrated to be ready for the deployment in automated CFRP manufacturing processes. Further research work will investigate the performances of FBG sensors written on bend-insensitive fibers after embedding into CFRP structures.

5 ACKNOWLEDGEMENTS

The authors would like to acknowledge the support of Dr Paolo Proli for the manufacturing of the specimens in autoclave. The work was done in collaboration with Riba Composites, an Italian well-established company manufacturing advanced composite structures for the marine, automotive and aerospace industry fields.

6 REFERENCES

[1] de Oliveira, R., Ramos, C.A. and Marques, A.T., “Health monitoring of composite structures by embedded FBG and interferometric Fabry-Pérot sensors”, Comput. Struct. 86, 340-346 (2008).

[2] Di Sante, R., and Scalise, L., “A single-mode optical fiber interferometer for surface vibration measurement” Proc. SPIE 4204, p. 115, Newport (2001).

[3] Di Sante, R. and Scalise, L. “Multipoint optical fiber vibrometer”, Rev. Sci. Instrum. 73, p. 1321 (2002).

[4] Di Sante, R. and Scalise, L., "A novel fiber optic sensor for multiple and simultaneous measurement of vibration velocity", Rev. Sci. Instrum. 75, p. 1952 (2004).
[5] De Baere, I., Voet, E., Van Paepegem, W., Vlekken, J., Cnudde, V., Masschaele, B. and Degrieck, J., "Strain monitoring in thermoplastic composites with optical fiber sensors: Embeddig process, visualization with micro-tomography and fatigue results, J. Thermoplast. Compos. Mater. 20, p. 453 (2007).
[6] Luycks, G., Voet, E., Lammens, N. and Degrieck, J., "Strain measurements of composite laminates with embedded fibre Bragg gratings: criticism and opportunities for research", Sensors 11, p. 384 (2011).
[7] Abe, I., Kalinowski, H.J., Frazao, O., Santos, J.L., Nogueira, R.N. and Pinto, J.L., "Superimposed Bragg gratings in high-birefringence fibre optics: three-parameter simultaneous measurements", Proc. of 16th Int. Conf. on Opt. Fibre Sensor (OFS-16), p. 1453, Nara City, Japan (2003).
[8] R. Di Sante, L. Donati, E. Troiani e P. Proli, "Strain monitoring in advanced composite structures for nautical applications", International Union of Materials Research Society – International Conference in Asia 2012, IUMRS-ICA 2012, Busan, Korea, August 26-31, 2012.